Bull. Inst. Chem. Res., Kyoto Univ., Vol. 49, No. 4, 1971

Sedimentation Equilibrium in Nonideal Heterogeneous System II. Remarks on Hinge-Point Analysis

Nobuo DONKAI and Tadao KOTAKA*

Received May 31, 1971

A sedimentation-equilibrium procedure proposed by Van Holde, Baldwin, and Yphantis was extended to treat nonideal solutions of heterogeneous solutes. The procedure is based on the use of original concentration and a single value of concentration gradient at a particular location where the local equilibrium concentration coincides with the original solute concentration (the *hinge-point*). The method involves two approaches: In the midpoint approach, the hinge-point is replaced by the midpoint that is easier to be located; and in the meniscus depletion approach, the method is combined with meniscus depletion technique. Dependences of experimentally observable molecular weights on solute-concentration and on sedimentation parameter λ are discussed.

In the former, the average molecular weight and the apparent second virial coefficient obtained in the limit of infinite dilution depend on the parameter λ, *i. e.*, both are decreasing functions of increasing λ: In the limit of λ being zero, the former becomes a type of weight average molecular weight and the latter a type of light-scattering second virial coefficient. Whereas in the meniscus depletion approach, since λ must be sufficiently large so as to achieve the condition of meniscus depletion, the observable molecular weight is very sensitive to the solute heterogeneity. The meniscus depletion method appears to become less practical for heterogeneous solute systems.

INTRODUCTION

In contrast to conventional sedimentation equilibrium analysis that is based on the observation of solute distribution in entire solution column at the sedimentation-diffusion equilibrium,[1] there is a different type of procedure proposed by Van Holde and Baldwin[2] that is based on the use of original solute-concentration and value of concentration gradient at one particular location in the cell. The position may be called the *hinge-point*, where the local-equilibrium concentration is equal to the original concentration of the solution. The method has been advanced by Yphantis[3] incorporating multichannel cells, and is now in current use. As the method stands now, it involves two different approaches. In one approach, one chooses rather low centrifugation speed and very short column height, say around 1 mm, and utilizes the value of concentration gradient at the midpoint, instead of that at the exact hinge-point of the solution column.[2,3a] In other approach, one employs high centrifugation speed so that the meniscus concentration of solute goes to zero, and then utilizes the value of concentration gradient at the exact hinge-point.[3b] The location can be easily determined, when the meniscus concentration is zero.

* 呑海　信雄, 小高　忠男: Laboratory of Macromolecular Characterization, Institute for Chemical Research, Kyoto University, Uji, Kyoto.

These approaches have certain features of advantage, particularly upon dealing with monodisperse solute systems: For example, the method is rapid and, hence, is suitable to dealing with high molecular weight materials. The data processing is very simple, although the accuracy is admittedly poor. Because of these features, it would be interesting and worthwhile to examine the performance of the method, when it is applied to more general case of nonideal solutions of heterogeneous solute systems.

In a preceding article[4] we developed fundamental equations on sedimentation equilibrium behavior of nonideal, heterogeneous systems. In this article we apply the equations to describe the *hinge-point* analysis of such systems. The results will be compared with experimental data obtained on a few special cases.

THEORY

For the hinge-point analysis, observable molecular weight $\bar{M}_\dagger^{app}$ is defined as follows:[2,3]

$$\bar{M}_\dagger^{app}=\frac{RT}{(1-\bar{v}^\circ\rho_s)\omega^2}\frac{1}{\tilde{n}^\circ}\left(\frac{1}{r}\frac{d\tilde{n}}{dr}\right)_{r=r_\dagger} \tag{1a}$$

$$=(1/\lambda\tilde{n}^\circ)(d\tilde{n}/dx)_{x=x_\dagger} \tag{1b}$$

The subscript $r=r_\dagger$ (or $x=x_\dagger$) indicates that the quantity in the bracket is to be taken at the hinge-point $r_\dagger$ (or $x_\dagger$ in reduced scale). The sedimentation parameter λ, reduced radial distance x, original and local-equilibrium concentrations of the solution, $\tilde{n}^\circ$ and $\tilde{n}$, measured in refractometric scale are defined, respectively, as follows:

$$\lambda=(1-\bar{v}^\circ\rho_s)\omega^2(b^2-a^2)/2RT \tag{2a}$$

$$x=(r^2-a^2)/(b^2-a^2) \tag{2b}$$

$$\tilde{n}^\circ=\nu^\circ c^\circ=\sum\nu_i c_i^\circ\ ;\quad \tilde{n}=\nu c=\sum\nu_i c_i \tag{2c, d}$$

The abbreviations used are as follows: RT, the gas constant times the absolute temperature; ω, angular speed of rotation; $\bar{v}^\circ$, the average partial specific volume of solutes in the original solution; ρ_s, the solvent density; r, a and b, the radial distances to a given position, to the meniscus and to the bottom of the solution column, respectively; ν_i and ν, the specific refractive increment of solute i and its local average value, respectively; c_i° and c_i, the original and the local-equilibrium concentrations of solute i, respectively. The superscript $\circ$ denotes quantities referred to the original solution.

In the previous article,[4] we gave a differential equation describing equilibrium distribution of solue i in a heterogeneous q-solute system, together with the conservation of mass statement. The equations read

$$\lambda M_i^*\theta_i=(d\theta_i/dx)+\lambda c^\circ\sum_k(M_iM_k^*\bar{B}_{ik}J_{ik})\gamma_k^\circ \tag{3a}$$

$$M_i^*=[(1-\bar{v}_i\rho_s)/(1-\bar{v}^\circ\rho_s)]M_i=(\beta_i/\beta^\circ)M_i \tag{3b}$$

$$\theta_i=c_i/c_i^\circ\ ;\quad \gamma_k^\circ=c_k^\circ/c^\circ \tag{3c, d}$$

$$\bar{B}_{ik}=B_{ik}+\bar{v}_i/M_k \tag{3 e}$$

$$J_{ik}=(\lambda M_k^*)^{-1}\theta_i(d\theta_k/dx) \tag{3 f}$$

$$\int_0^1\theta_i\,dx=1\,;\ (0\leqq x\leqq 1\,;\quad i,\,k=1,\,2,\cdots,\,q) \tag{4}$$

Here β_i is the apparent bouyancy factor of solute i as defined by eq. (3 b) with $\bar{v}_i$ being its partial specific volume; θ_i and γ_k^0 are the relative equilibrium distribution of solute i and the relative abundance of solute k in the original solution, respectively; B_{ik} is the i-k interaction parameter.

Combining eqs. (1), (2) and (3), we obtain an expression for observable molecular weight $\bar{M}_\dagger^{app}$ as

$$\bar{M}_\dagger^{app}=\lambda^{-1}\sum[(\nu_i/\nu^\circ)(d\theta_i/dx)_{x=x_\dagger}]\gamma_i^\circ \tag{5 a}$$

$$=\sum\tilde{M}_i^*\theta_i(x_\dagger)\gamma_i^\circ-c^\circ\sum\sum[\tilde{M}_iM_k^*\bar{B}_{ik}J_{ik}(x_\dagger)]\gamma_i^\circ\gamma_k^\circ \tag{5 b}$$

The hinge-point is, according to its definition, to be a position wherein $\sum\theta_i(x_\dagger)\times\gamma_i^\circ=1$. However, for a heterogeneous solute system which consists of solutes with different ν, there is no way of locating the exact hinge-point. In stead it can be located only in the refractometric scale. Wherein the following identity holds:

$$\sum(\nu_i/\nu^\circ)\theta_i(x_\dagger)\gamma_i^\circ=1 \tag{6}$$

Apparently at any point all θ_i do not simultaneously become unity, except in the limit of λ infinitely approaching zero. In that sense, the first term in the right-hand-side of eq. (5 b) is dependent on λ as well as c°, and in addition, on the way how one locates or approximates the hinge-point. The situation is entirely different from that of conventional equilibrium analysis.

First assuming that c° is sufficiently small, we expand the term $\theta_i(x_\dagger)$ in powers of c°:[4]

$$\theta_i(x_\dagger)=\theta_i^{\dagger(0)}+c^\circ\theta_i^{\dagger(1)}+(c^\circ)^2\theta_i^{\dagger(2)}+\cdots \tag{7 a}$$

$$\theta_i^{\dagger(0)}=A_i\exp(\lambda M_i^*x_\dagger) \tag{7 b}$$

$$A_i=\lambda M_i^*/[\exp(\lambda M_i^*)-1] \tag{7 c}$$

$$\theta^{\dagger(1)}=\theta_i^{\dagger(0)}\sum_k M_i\bar{B}_{ik}[(A_iA_k/A_{ik})-\theta_k^{\dagger(0)}]\gamma_k^\circ \tag{7 d}$$

$$A_{ik}=\lambda(M_i^*+M_k^*)/[\exp\{\lambda(M_i^*+M_k^*)\}-1] \tag{7 e}$$

etc. Then, from eqs. (5) and (7) we obtain

$$\bar{M}_\dagger^{app}=\sum\tilde{M}_i^*\theta_i^{\dagger(0)}\gamma_i^\circ$$
$$-c^\circ\sum\sum\tilde{M}_i\bar{B}_{ik}\theta_i^{\dagger(0)}[(M_i^*+M_k^*)\theta_k^{\dagger(0)}-M_i^*(A_iA_k/A_{ik})]\gamma_i^\circ\gamma_k^\circ$$
$$+0[(c^\circ)^2] \tag{8}$$

Apparently, even in the limit of c° being zero, the quantity $\bar{M}_\dagger^{app}$ is still dependent on λ through $\theta_i^{\dagger(0)}$, and tend to a value giving a type of weight average molecular weight only when λ also approaches zero. In such a case, the λ-dependent terms in the c°-expansion coefficients of $\bar{M}_\dagger^{app}$ may be expanded in powers of λ:

$$\theta_i^{\dagger(0)}=1+(\lambda M_i^*)(x_\dagger-1/2)+(\lambda M_i^*)^2[(x_\dagger-1/2)^2/2-1/24]$$
$$+(\lambda M_i^*)^3[x_\dagger(x_\dagger-1/2)(x_\dagger-1)/6]+0[(\lambda M_i^*)^4] \quad (9\,a)$$
$$A_iA_k/A_{ik}=1+(\lambda^2/12)M_i^*M_k^*+0(\lambda^4) \quad (9\,b)$$

etc. The combination of eqs. (8) and (9) leads to

$$\bar{M}_\dagger^{app}=\bar{M}_\dagger(\lambda)-(\bar{M}_1)^2c^\circ B_\dagger^{app}F_\dagger(\lambda)+\cdots \quad (10\,a)$$
$$\bar{M}_\dagger(\lambda)=\bar{M}_1\{1+\lambda(x_\dagger-1/2)\bar{M}_{2/1}-(\lambda^2/24)[1-2(x_\dagger-1/2)^2]\bar{M}_{2/1}\bar{M}_{3/2}+\cdots\} \quad (10\,b)$$
$$B_\dagger^{app}F_\dagger(\lambda)=B_{2/2}+2\lambda(x_\dagger-1/2)(\bar{M}_{2/1})^2B_{4/4}$$
$$-(\lambda^2/24)\{(\bar{M}_{2/1})^2+4\bar{M}_{2/1}\bar{M}_{3/2}-12(x_\dagger-1/2)^2[3(\bar{M}_{2/1})^2+4\bar{M}_{2/1}\bar{M}_{3/2}]\}B_{4/4}$$
$$+0(\lambda^3) \quad (10\,c)$$

Here $\bar{M}_1$, $\bar{M}_{2/1}$, $\bar{M}_{3/2}$ *etc.* are the average molecular weights giving, respectively, a type of weight-average, z-average, $(z+1)$-average *etc.*, and are defined as[2,4]

$$\bar{M}_1=\sum\tilde{M}_i^*\gamma_i^\circ \quad (11\,a)$$
$$\bar{M}_{2/1}=(\bar{M}_1)^{-1}\sum\tilde{M}_i^*(M_i^*)\gamma_i^\circ \quad (11\,b)$$
$$\bar{M}_{3/2}=(\bar{M}_1\bar{M}_{2/1})^{-1}\sum\tilde{M}_i^*(M_i^*)^2\gamma_i^\circ \quad (11\,c)$$

etc., and $B_{2/2}$, $B_{4/4}$ *etc.* are the average second virial coefficients defined, respectively, as follows:[4,5]

$$B_{2/2}=(\bar{M}_1)^{-2}\sum\sum\tilde{M}_iM_k^*\bar{B}_{ik}\gamma_i^\circ\gamma_k^\circ \quad (11\,d)$$
$$B_{4/4}=(\bar{M}_1\bar{M}_{2/1})^{-2}\sum\sum\tilde{M}_iM_k^*(M_i^*M_k^*)\bar{B}_{ik}\gamma_i^\circ\gamma_k^\circ \quad (11\,e)$$
$$\cong(\bar{M}_1)^{-2}(\bar{M}_{2/1}\bar{M}_{3/2})^{-1}\sum\sum\tilde{M}_iM_k^*(M_i^*)^2\bar{B}_{ik}\gamma_i^\circ\gamma_k^\circ \quad (11\,f)$$
$$\cong(\bar{M}_1)^{-2}(\bar{M}_{2/1}\bar{M}_{3/2})^{-1}\sum\sum\tilde{M}_iM_k^*(M_k^*)^2\bar{B}_{ik}\gamma_i^\circ\gamma_k^\circ \quad (11\,g)$$

Here the quantity $B_{2/2}$ is a type of light-scattering second virial coefficient, as defined before.[4,5] Strictly speaking, the quantities defined by eqs. (11 e), (11 f) and (11 g) differ slightly from one another. However, the difference appears to be trivial, and hence we assigned the same symbol $B_{4/4}$ to all three of them. The quantity $B_{4/4}$ in the λ^2-term of eq. (10 c) involves these three different averages.

Generally the type of average molecular weight obtained by extrapolating $\bar{M}_\dagger^{app}$ to infinite dilution depends on the approximation employed for locating the hinge-point. We discuss below on the two approaches, *i. e.*, the midpoint approach and the meniscus-depletion approach.

Midpoint Approach: In this procedure one usually employs a condition so as to λ being sufficiently small. In that case the expansion forms, eqs. (10 a) (10 c) may be used as the starting equations. It should be noted that all the terms with odd powers of λ in eqs. (10 b) and (10 c) involve a multiplier $(x_\dagger-1/2)$. Therefore, if we replace the hinge-point $x_\dagger$ by the midpoint x_m

$$x_m=x=1/2, \text{ or } r_m=r=[a^2+(1/2)(b^2-a^2)]^{1/2} \quad (12\,a, b)$$

the odd power terms of λ identically vanish. Then, the quantity $\bar{M}^{app}$ may be recast into a simple form $\bar{M}_m^{app}$ as

$$(\bar{M}_m{}^{app})^{-1}=(\bar{M}_m)^{-1}+c^\circ B_m{}^{app}F_m(\lambda)+\cdots \tag{13 a}$$

$$\bar{M}_m=\bar{M}_\dagger(x_\dagger=1/2)=\sum\tilde{M}_i^*[(\lambda M_i^*/2)/\sinh(\lambda M_i^*/2)]\gamma_i^\circ \tag{13 b}$$

$$=\bar{M}_1\{1-(\lambda^2/24)\bar{M}_{2/1}\bar{M}_{3/2}+(7\lambda^4/5760)\bar{M}_{2/1}\bar{M}_{3/2}\bar{M}_{4/3}\bar{M}_{5/4}+0(\lambda^6)\} \tag{13 c}$$

$$B_m{}^{app}F_m(\lambda)=B_{2/2}-(\lambda^2/24)\{[(\bar{M}_{2/1})^2+4\bar{M}_{2/1}\bar{M}_{3/2}]B_{4/4}-2\bar{M}_{2/1}\bar{M}_{3/2}B_{2/2}\}+0(\lambda^4) \tag{13 d}$$

Apparently the observable molecular weight $\bar{M}_m{}^{app}$ yields $\bar{M}_1$ and $B_{2/2}$ only after dual extrapolation with respect to both c° and λ^2. It should be noted that the apparent second virial coefficient, eq. (12 c), is expected to decrease with increasing λ^2, as opposed to that of $(\bar{M}_1{}^{app})^{-1}$ versus c° plot obtained in the conventional analysis.[4]

Meniscus-Depletion Approach: In this procedure, one employs a condition of high-speed centrifugation (*i. e.*, of large λ) so that concentrations of all solutes go to zero at the meniscus, $\theta_i(0)=0$ for all i. Then, one locates the (refractometric) hinge-point $x_\dagger$ by integrating area under the schlieren gradient curve or by simply measuring displacement of the Rayleigh fringe pattern. Theoretically $x_\dagger$ is obtained by solving eq. (6) : The problem is very difficult to be carried through. Therefore, we discuss here the behavior in a limiting case wherein the effects of nonideality are negligible. For heterogeneous solute systems, the Flory theta condition[6] is unlikely to exist, and the assumption of vanishing nonideality would be valid only in the limit of infinitely high dilution. With these stipulations, the observable molecular weight $\bar{M}_\dagger{}^{app}$ and the condition for locating the hinge-point may be given, respectively, as

$$\bar{M}_\dagger{}^{app}=\sum\tilde{M}_i^*\theta_i{}^{\dagger(0)}\gamma_i^\circ \tag{14 a}$$

$$\sum(\nu_i/\nu^0)\theta_i{}^{\dagger(0)}\gamma_i{}^0=1 \tag{14 b}$$

Another problem to be solved is that, because of the condition of meniscus-depletion, eq. (14 a) cannot be expanded in powers of λ. Instead, we assume that there must be a solute "†" and its hinge-point coincides with that of the whole solute, *i. e.*, $1=\theta_\dagger{}^{\dagger(0)}$. Then solving this relation, we obtain

$$x_\dagger=1+(\lambda M_\dagger^*)^{-1}\{\ln[1-\exp(-\lambda M_\dagger^*)]-\ln(\lambda M_\dagger^*)\} \tag{15 a}$$

On the other hand, the condition of the meniscus depletion demands that the value λM_i^* should be large enough so as to the factor $\exp(-\lambda M_i^*)$ being negligible for all components i. Taking all these requirements into account, we obtain an expression of $\theta_i{}^{\dagger(0)}$ as

$$\theta_i{}^{\dagger(0)}=(M_i^*/M_\dagger^*)(\lambda M_\dagger^*)^{(1-M_i^*/M_\dagger^*)} \tag{15 b}$$

Combining eqs. (14 a, b) and (15 b), we obtain

$$\bar{M}_\dagger{}^{app}=\frac{\sum[\tilde{M}_i^*(M_i^*)(\lambda M_\dagger^*)^{(1-M_i^*/M_\dagger^*)}]\gamma_i^\circ}{\sum[\tilde{M}_i^*(\lambda M_\dagger^*)^{(1-M_i^*/M_\dagger^*)}]\gamma_i^\circ} \tag{16}$$

The quantity $\bar{M}_\dagger{}^{app}$ is a complex average molecular weight: If the factor, $(\lambda M_\dagger^*)^{(1-M_i^*/M_\dagger^*)}$, may be approximated as unity, the value becomes a type of z-average, $\bar{M}_{2/1}$. Usually the factor is a decreasing function of M_i^*, and hence,

the $\bar{M}_\dagger^{app}$ should be a lower-order average than the z-average.

When the solute heterogeneity is negligibly small, *i.e.*, $|1-M_i^*/M_\dagger^*| \ll 1$ for all i, the factor may be approximated as unity:

$$(\lambda M_\dagger^*)^{(1-M_i^*/M_\dagger^*)} = 1+(1-M_i^*/M_\dagger^*)\ln(\lambda M_\dagger^*)+[(1-M_i^*/M_\dagger^*) \times \ln(\lambda M_\dagger^*)]^2+\cdots \quad (17\,a)$$

Then the observable molecular weight $\bar{M}_\dagger^{app}$ becomes

$$\bar{M}_\dagger^{app} = \bar{M}_{2/1}\frac{1+(1-\bar{M}_{3/2}/M_\dagger^*)\ln(\lambda M_\dagger^*)+\cdots}{1+(1-\bar{M}_{2/1}/M_\dagger^*)\ln(\lambda M_\dagger^*)+\cdots} \quad (17\,b)$$

On the other hand, the quantity $M_\dagger^*$ may be given by solving the condition of the hinge-point, *i.e.*, eq. (14 b):

$$M_\dagger^* = \sum[\tilde{M}_i^*(\lambda M_\dagger^*)^{(1-M_i^*/M_\dagger^*)}]\gamma_i^\circ \quad (18\,a)$$

Here we apply the same approximation of negligible solute-heterogeneity, and replace the quantity $M_\dagger^*$ by $\bar{M}_1$, neglecting the higher order terms in the right-hand-side of eq. (17 a). Then we obtain

$$\bar{M}_\dagger^{app} = \bar{M}_{2/1}\{1-[(\bar{M}_{3/2}-\bar{M}_{2/1})/\bar{M}_1]\ln(\lambda\bar{M}_1)+\cdots\} \quad (18\,b)$$

Apparently the quantity $\bar{M}_\dagger^{app}$ is quite sensitive to the solute-heterogeneity and the sedimentation parameter λ. It should be reminded that the value of λ should be chosen to be sufficiently large so that $\lambda\bar{M}_1$ is about 7~10 or more, because of the requirement of the meniscus depletion. Consequently a slightest heterogeneity of solute would make the method to be rather impractical.

COMPARISON WITH EXPERIMENTAL RESULTS

Experimental Procedures

The procedure and the materials used were the same as those described in the previous article.[4] However, in this case, most of the sedimentation patterns were recorded on a schlieren optics with a phase angle of 75°. Besides a Yphantis 6-channel cell, we used an 8-channel circular cell with 12 mm thickness.[3] Otherwise the procedures were the same as before.[4] The materials used were also the same; a monodisperse polystyrene PST-1 a, a polydisperse poly (methyl methacrylate) PMMA-31 M, and a blend of the two polymers (PST-1 a : PMMA-31 M = 0.499_7 : 0.500_3 by weight). The solvent was 2-butanone (MEK). The characterization data of the polymer samples are listed in Table 1.

Table 1. Characterization Data of Polymer Samples.

Code	$10^{-4}M_n$	$10^{-4}M_w$	Sedimentation Equilirium Data[a]		
			$10^{-4}\bar{M}_1$	$10^4 B^{app}$	$10^{-4}\bar{M}_{2/1}$
PST-1 a	15.5	16.0	16.3	2.9	16.6
PMMA-31 M	16.6	20.0	20.4	7.4	22.6
1 : 1 blend	—	—	19.1	7.9	20.8

a) Data in MEK at 25°C obtained by the conventional analysis (ref. 4). Values of $\bar{M}_1$ and $\bar{M}_{2/1}$ become equal to M_w and M_z, respectively, for homologous polymer samples; the B^{app} is the second virial coefficient determined from $(\bar{M}_1^{app})^{-1}$ versus $\tilde{c}$ plot.

Application to Special cases

Two component system: For a two component system with the solute molecular weight M and the second virial coefficient B, observable molecular weight $\bar{M}_\dagger^{app}$ may be expressed as

$$(\bar{M}_\dagger^{app})^{-1}=[M\theta(x_\dagger)]^{-1}[1+Mc^\circ B\theta(x_\dagger)] \tag{19 a}$$

Here $\theta(x_\dagger)$ is the value of the relative equilibrium distribution of solute at the hinge-point $x_\dagger$. It must be unity for a two component system, if the exact location of $x_\dagger$ is taken. The location may be determined without much difficulty, and then, the $\bar{M}_\dagger^{app}$ becomes

$$(\bar{M}_\dagger^{app})^{-1}=M^{-1}+c^\circ B \tag{19 b}$$

The equation (19 b) applies to the meniscus depletion approach as well.

On the other hand, if $x_\dagger$ is replaced by the midpoint $x_m=1/2$, the quantity $\theta(x_m)$ is not necessarily unity. The theoretical value of $\theta(x_m)$ may be calculated easily, for example, by applying c°-series expansion method.[1c,4] With these solutions and eq. (19 a), we obtain

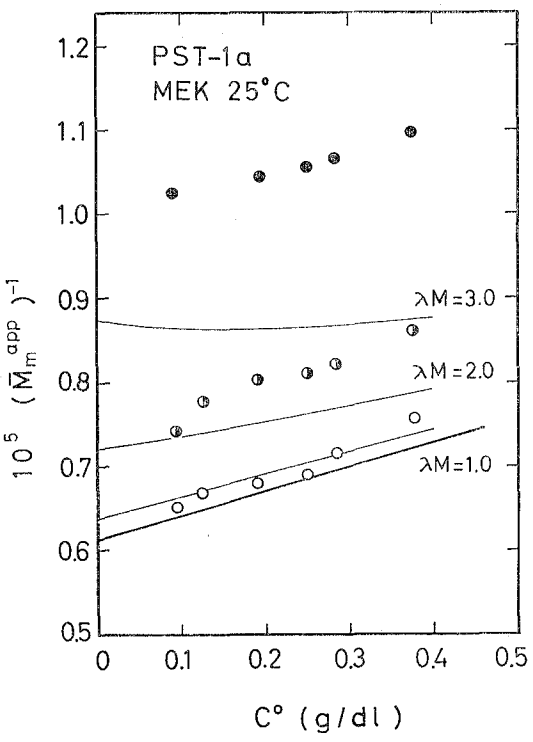

Fig. 1. Plots of reciprocal (midpoint) apparent molecular-weight $(\bar{M}_m^{app})^{-1}$ versus original solution concentration c^0 for nearly monodisperse PST-1 a in MEK at 25°C: values of λM_w range 0.97-1.12 (white circles); 1.82-2.11 (half-black circles); and 3.02-3.49 (black circles) for the three sets of data. Heavy line represents the conventional M_w-plot,[4] into which the present plots should merge at the limit of λM being zero; thin lines represent the theoretical curves as computed by eq. (20 a) with the value of λM as indicated.

$$(\bar{M}_m^{app})^{-1} = (\bar{M}_m)^{-1} + c^\circ B f_m(\lambda) + \cdots \quad (20\,a)$$

$$\bar{M}_m = M[(\lambda M/2)/\sinh(\lambda M/2)] \quad (20\,b)^{2,3)}$$

$$f_m(\lambda) = 1 - [\cosh(\lambda M/2) - 1] \quad (20\,c)$$

In the limit of λ being zero, the factor $(\lambda M/2)/\sinh(\lambda M/2)$ approaches unity and the factor $[\cosh(\lambda M/2)-1]$ to zero, thus the right-hand-side of eq. (20 a) becomes equal to that of eq. (19 b).

Numerical calculation of eq. (20 a) was carried out upto the $(c^\circ)^3$-term. The results are compared with experimental data obtained on PST-1a in MEK at 25°C, as demonstrated in Fig. 1. As anticipated, both $\bar{M}_m$ and $Bf_m(\lambda)$ are highly dependent on λM. For example, at $\lambda M = 1.5$ that is the value usually encountered in experiments, the deviation of $\bar{M}_m$ from exact M amounts to about 10%. In such a case, eq. (20 b) may be used to estimate exact M. It is noticeable that the apparent slope of the plots becomes nearly zero around $\lambda M = 3$ in this system.

Homologous polymer system: For this system, we assume as before[4] that all components have the same values of $\nu_i = \nu$ and $\bar{v}_i = \bar{v}^\circ$, and that all $\bar{B}_{ik}$'s are the same as B. Then, it is easy to rewrite eqs. (13 a)-(13 d) to obtain $\bar{M}_m^{app}$:

$$(\bar{M}_m^{app})^{-1} = (\bar{M}_m)^{-1} + c^\circ B \bar{F}_m(\Lambda) + \cdots \quad (21\,a)$$

$$\bar{M}_m = M_w\{1 - (\Lambda^2/24)p_z p_{z+1} + (7\Lambda^4/5760)p_z p_{z+1} p_{z+2} p_{z+3} + 0(\Lambda^6)\} \quad (21\,b)$$

$$\bar{F}_m(\Lambda) = 1 - (\Lambda^2/24)p_z(p_z + 2p_{z+1}) + 0(\Lambda^4) \quad (21\,c)$$

$$\Lambda = \lambda M_w\,;\ p_z = M_z/M_w,\ p_{z+1} = M_{z+1}/M_w,\ etc. \quad (21\,d)$$

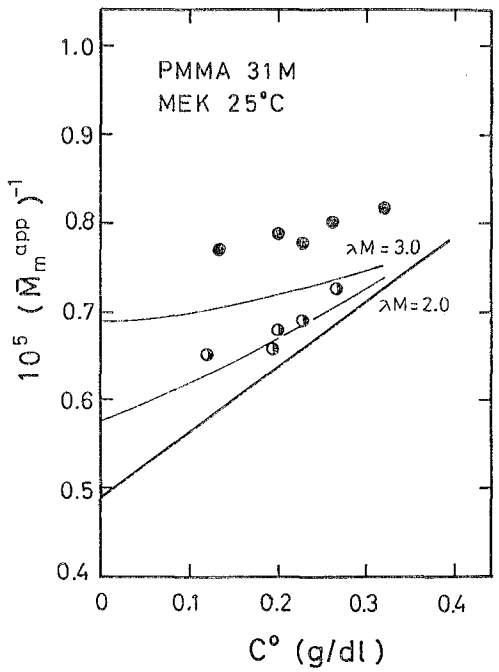

Fig. 2. Plots of $(\bar{M}_m^{app})^{-1}$ versus c^0 for polydisperse PMMA-31M in MEK at 25°C: values of λM_w range 1.70-2.08 (half-black circles) and 2.64-2.95 (black circles) for the two sets of data. For other symbols, see Fig. 1.

On the other hand, the observable molecular weight $\bar{M}_{\dagger}^{app}$ based on the meniscus depletion method may be written as

$$(\bar{M}_{\dagger}^{app})^{-1}=[M_z\{1-(p_{z+1}-p_z)\ln+\cdots\}]^{-1}+0(c^{\circ}) \qquad (22)$$

As noted in the previous section, the c°-independent term of $\bar{M}_{\dagger}^{app}$ is highly sensitive to the solute heterogeneity and the sedimentation parameter λ: For example, since the parameter Λ must be chosen to be around 7~10 or larger, the solute heterogeneity of as small as $p_{z+1}-p_z=0.05$ would result in the reduction of $\bar{M}_{\dagger}^{app}$ by as large as 10 to 23% or more. In addition, its c°-dependent terms are also expected to be highly sensitive to the solute heterogeneity, although the exact feature has not yet been known. An application of the meniscus-depletion method would become less satisfactory for a solute with even a slightest heterogeneity.

The equations (21) and (22) are tested with data on PMMA-31M in MEK at 25°C. Fig. 2, shows the plots of $(\bar{M}_m^{app})^{-1}$ versus c°. The results are compared with theoretical curves of a two component system and also with the conventional $(\bar{M}_1^{app})^{-1}$ versus $\tilde{c}$ data for the same system.[4] The calculation was made by eq. (20 a) including upto the $(c^{\circ})^3$-terms, wherein M and B were identified respectively with M_w and B of this system.[4] Here the $\bar{M}_1^{app}$ is the observable molecular weight giving a type of wight average value and $\tilde{c}$ is the

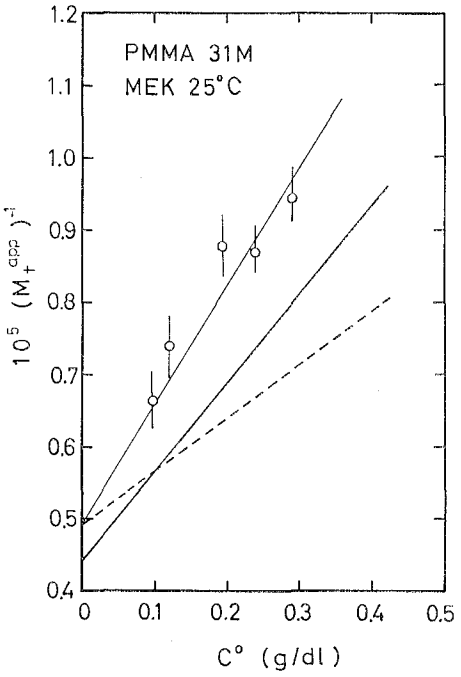

Fig. 3. Plots of reciprocal (meniscus-depletion) apparent molecular-weight $(M_{\dagger}^{app})^{-1}$ versus c^0 for PMMA-31M in MEK at 25°C: heavy dashed line represents the conventional M_w-plot, and heavy solid line the conventional M_z-plot.[4] Vertical line on each point indicates the error limit.

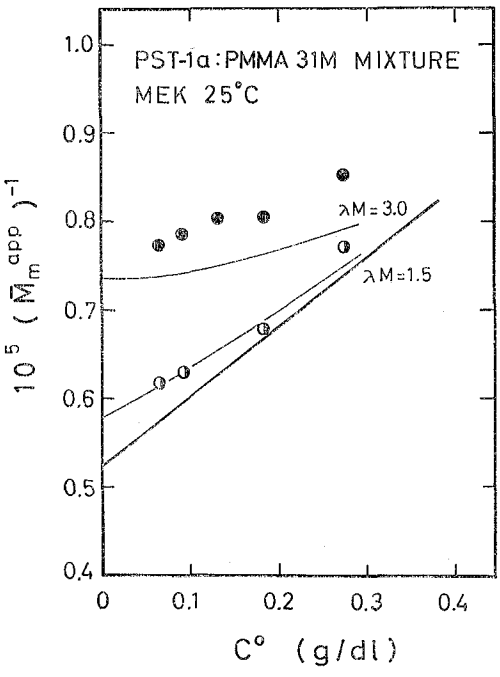

Fig. 4. Plots of $(\bar{M}_m^{app})^{-1}$ versus c^0 for the 1 : 1 blend of PST-1a and PMMA-31M in MEK at 25°C: values of λM_w range 1.36-1.58 (half-black circles) and 2.60-3.01 (black circles) for the two sets of data. For other symbols, see Fig. 1.

average concentration in the equilibrium solute distribution measured in refractometric scale.[2,4] The feature of the plots is similar to those of a two component system (cf., Fig. 1). The influence of varying λ on $\bar{M}_m$ and $\bar{F}_m(\Lambda)$ appears to be more significant in the polydisperse system than in the monodisperse system. When the value of λ is appropriately chosen so as to Λ being, say, about 1.5 or less, the midpoint method appears to provide reasonable estimates of M_w and B.

Figure 3, shows the plot of $(\bar{M}_\dagger^{app})^{-1}$ versus c° based on the meniscus-depletion approach. The plot is compared with the conventional $(\bar{M}_{2/1}^{app})^{-1}$ versus $\tilde{c}$ plot of the same system.[4] Here the $\bar{M}_{2/1}^{app}$ is the observable molecular weight giving a type of z-average value.[2,4] The heterogeneity of this sample has been estimated to be small[4] (cf., Table 1). Nevertheless, considerable descrepancy is observed between the two types of the plots.

Poly (A) : poly (B) blend : The equations (13) and (16) are tested with data on the PST-1a : PMMA-31M blend in MEK at 25°C. Figure 4, shows the plots of $(\bar{M}_m^{app})^{-1}$ versus c°, which are again compared with theoretical curves calculated under the two-component-system approximation and with the conventional plot of the same system.[4] Again the feature of the plots is quite similar to the previous two systems (cf., Fig. 1 and 2).

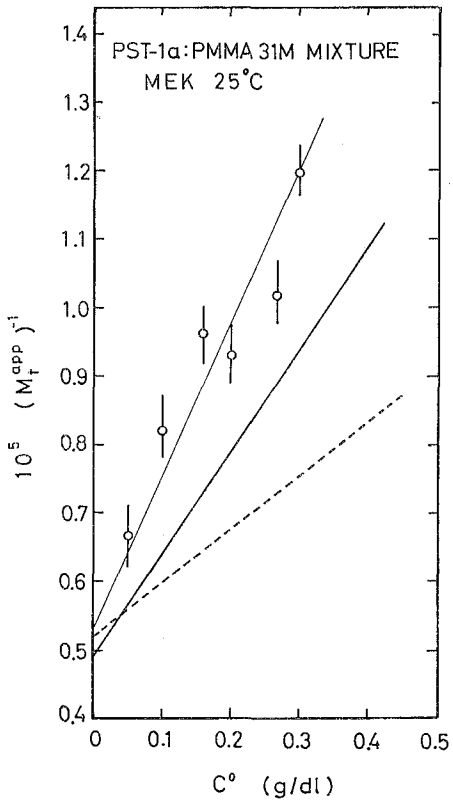

Fig. 5. Plots of $(M_\dagger^{app})^{-1}$ versus c° for the 1 : 1 blend of PST-1a and PMMA-31M in MEK at 25°C. For other symbols, see Fig. 3.

Figure 5, shows the plot of $(\bar{M}_{\dagger}^{app})^{-1}$ versus c° based on the meniscus-depletion method together with the conventional plots of $(\bar{M}_{2/1}^{app})^{-1}$ versus $\bar{c}$ of the same system.[4] Again we find considerable descrepancy between the two plots. In general the hinge-point method combined with meniscus depletion technique is quite sensitive to the solute heterogeneity, partly because of the requirement that the parameter λ should be sufficiently large. Hence the method appears to be less practical for heterogeneous solute systems. In fact the meniscus depletion method is more conveniently applied for monodisperse solute in ideal solution.[3b] In such cases, it is customary to plot the logarism of equilibrium solute concentration, ln $c(r)$, against the square of the radial distance, r^2: then the plot of ln $c(r)$ versus r^2 always gives a straight line and the solute molecular weight may be evaluated from the slope of the plot. However, for a nonideal solution of a heterogeneous solute the plot usually deviates from the linearity, reflecting both the heterogeneity and the nonideality of the solution in somewhat complicated manner. The problem will be discussed in a later publication.

ACKNOWLEDGMENT

We wish to thank Professor H. Inagaki for his encouragement and valuable discussion on this problem. One of us (T. K.) acknowledges a financial support from the Ministry of Education through grant A4037 in 1969-70.

REFERENCES

(1) See for example: (a) J. W. Williams, K. E. Van Holde, R. L. Baldwin, and H. Fujita, *Chem. Rev.*, 58, 715 (1958); (b) R. L. Baldwin and K. E. Van Holde, *Fortschr. Hochpolym. Forsch.*, 1, 451 (1960); (c) H. Fujita, "Mathematical Theory of Sedimentation Analysis," Academic Press, New York, 1962.
(2) K. E. Van Holde and R. L. Baldwin, *J. Phys. Chem.*, 62, 734 (1958).
(3) (a) D. A. Yphantis, *Ann. New York Acad. Sci.*, 88, 586 (1960):
(b) D. A. Yphantis, *Biochemistry*, 3, 297 (1964).
(4) T. Kotaka, N. Donkai, and H. Inagaki, *J. Polymer Sci.*, to be published.
(5) T. Kotaka, N. Donkai, H. Ohnuma, and H. Inagaki, *ibid.*, A2, 6, 1803 (1968).
(6) See for example: P. J. Flory, "Principles of Polymer Chemistry," Cornell Univ. Press, Ithaca, N. Y., 1953, Chapters 12 and 13.